Acta Pharmacologica Sinica (2013) 34: 681–690
 1671-4083/13 $32.00
www.nature.com/aps

Original Article

NVP-BEZ235, a novel dual PI3K/mTOR inhibitor, enhances the radiosensitivity of human glioma stem cells *in vitro*

Wen-juan WANG[1], Lin-mei LONG[1], Neng YANG[1], Qing-qing ZHANG[1], Wen-jun JI[1], Jiang-hu ZHAO[1], Zheng-hong QIN[1], Zhong WANG[2], Gang CHEN[2], Zhong-qin LIANG[1, *]

[1]*Department of Pharmacology, Medical School of Soochow University, Suzhou 215123, China;* [2]*Department of Neurosurgery, the First Affiliated Hospital of Soochow University, Suzhou 215123, China*

Aim: NVP-BEZ235 is a novel dual PI3K/mTOR inhibitor and shows dramatic effects on gliomas. The aim of this study was to investigate the effects of NVP-BEZ235 on the radiosensitivity and autophagy of glioma stem cells (GSCs) *in vitro*.
Methods: Human GSCs (SU-2) were tested. The cell viability and survival from ionizing radiation (IR) were evaluated using MTT and clonogenic survival assay, respectively. Immunofluorescence assays were used to identify the formation of autophagosomes. The apoptotic cells were quantified with annexin V-FITC/PI staining and flow cytometry, and observed using Hoechst 33258 staining and fluorescence microscope. Western blot analysis was used to analyze the expression levels of proteins. Cell cycle status was determined by measuring DNA content after staining with PI. DNA repair in the cells was assessed using a comet assay.
Results: Treatment of SU-2 cells with NVP-BEZ235 (10–320 nmol/L) alone suppressed the cell growth in a concentration-dependent manner. A low concentration of NVP-BEZ235 (10 nmol/L) significantly increased the radiation sensitivity of SU-2 cells, which could be blocked by co-treatment with 3-MA (50 μmol/L). In NVP-BEZ235-treated SU-2 cells, more punctate patterns of microtubule-associated protein LC3 immunoreactivity was observed, and the level of membrane-bound LC3-II was significantly increased. A combination of IR with NVP-BEZ235 significantly increased the apoptosis of SU-2 cells, as shown in the increased levels of BID, Bax, and active caspase-3, and decreased level of Bcl-2. Furthermore, the combination of IR with NVP-BEZ235 led to G_1 cell cycle arrest. Moreover, NVP-BEZ235 significantly attenuated the repair of IR-induced DNA damage as reflected by the tail length of the comet.
Conclusion: NVP-BEZ235 increases the radiosensitivity of GSCs *in vitro* by activating autophagy that is associated with synergistic increase of apoptosis and cell-cycle arrest and decrease of DNA repair capacity.

Keywords: human glioblastoma; glioma stem cells; irradiation; radiosensitivity; apoptosis; autophagy; LC3; PI3K/mTOR pathway; NVP-BEZ235; 3-MA; cell cycle arrest; DNA repair

Acta Pharmacologica Sinica (2013) 34: 681–690; doi: 10.1038/aps.2013.22; published online 22 Apr 2013

Introduction

Human glioblastoma (GBM) is the most aggressive intracranial neoplasm in adults. Despite the current standard multimodal therapies, such as surgical resection, radiotherapy, and chemotherapy, the outcome for patients with GBM remains poor due to dismal prognosis and poor median survival. Understanding how these glioma cells develop and relapse might provide opportunities for the development of new therapies. Only a subpopulation of malignant glioma cells has true radio-chemoresistance and tumorigenic potential. This subpopulation of cells, called glioma stem cells (GSCs), reside in the stem-cell niche in the subventricular zone after ionizing radiation (IR)[1, 2]. GSCs are considered "seed" cells and have the capacity for selfrenewal, multipotent differentiation, and proliferation[3, 4]. Interestingly, GSCs are more radioresistant than primary tumor cells and could be responsible for tumor recurrence after radiation[5, 6]. Even though surgical therapy and radiotherapy kill a majority of glioma cells, they do not eliminate GSCs. Therefore, GSCs are the new cellular targets, and their eradication could prevent tumor recurrence.

GSCs can be eliminated in several ways: by employing sonic hedgehog signaling inhibitors in the stemness signature of GBM, by targeting the differentiation pathways, by delivering RNA interference (RNAi) to GBM cells, and by targeting the hyperactive cell cycle checkpoint kinases (Chk1 and Chk2)[7, 8]. The mammalian target of the rapamycin (mTOR)

* To whom correspondence should be addressed.
E-mail liangzhongqin@suda.edu.cn
Received 2012-11-19 Accepted 2013-02-26

inhibitor, rapamycin, induces autophagy and significantly affects the regulation of self-renewal, differentiation, tumorigenic potential, and radiosensitization of GSCs[9]. Autophagy can also be induced by transfecting GSCs with DNA-PKcs-RNAi after IR[10]. Therefore, we proposed that the defect in autophagy in GSCs contributes to the radioresistance of stem cells. The phosphatidylinositol 3-kinase (PI3K)/mTOR signaling pathway could be an effective therapeutic target for GBM. The PI3K/mTOR signaling pathway primarily affects diverse cellular functions, including proliferation, growth, differentiation, and survival[11]. This pathway also promotes tumor survival after radiation-induced DNA damage[12]. Dysregulation of this pathway is frequently observed in GBM and occurs via multiple mechanisms, including mutation of the *PIK3CA* gene[13], deregulation of mTOR complexes[14], and loss or mutation of the phosphatase and tensin homolog[15]. Inhibition of this cascade can enhance radiosensitivity of the tumor cells without affecting the normal cells, which is an attractive concept for improving therapeutic outcomes[16]. Therefore, inhibition of the PI3K/mTOR signaling pathway should be investigated as a strategy for treating GBM, and stem-like cells should be taken into consideration. NVP-BEZ235, a novel dual PI3K/mTOR inhibitor, showed a dramatic effect on gliomas in various laboratory-based testing approaches. NVP-BEZ235 antagonizes the PI3K/mTOR signaling pathway and induces cell-cycle arrest, autophagy, and downregulation of vascular endothelial growth factor in glioma cells[17]. NVP-BEZ235 is also an effective radiosensitizer that inhibits ataxia telangiectasia mutated (ATM) and DNA-PK catalytic subunits (DNA-PKcs), arrests cell cycle, and induces apoptosis[18–20]. Moreover, one of the stem-like cell lines, A172 cells, can be induced to undergo differentiation by pretreatment with NVP-BEZ235 and can produce a significant decrease in tumorigenicity when transplanted either subcutaneously or intracranially[21, 22].

Nevertheless, the effect of combined IR and NVP-BEZ235 treatments on the radioresistance of GSCs has not yet been reported. In this study, we examined the potential radiosensitization effect of NVP-BEZ235 on GSCs obtained from surgical specimens of recurrent gliomas[23] as well as its possible mechanisms.

Materials and methods

Cell culture

Human GSCs, which were named SU-2, were obtained and generated as described previously[23]. The cells were grown at 37 °C in the presence of 5% CO_2 in serum-free Dulbecco's modified Eagle's medium (DMEM)/F12 (Gibco Life Technologies, Paisley, UK) supplemented with recombinant human fibroblast growth factor (20 ng/mL; Invitrogen), recombinant human epidermal growth factor (20 ng/mL; Invitrogen), and N2 supplement (Gibco Life Technologies).

Reagents

NVP-BEZ235 was purchased from Selleck Chemicals and dissolved in dimethyl sulfoxide (DMSO; Sigma Aldrich, St Louis, MO) to obtain a stock concentration of 10 mmol/L, which was aliquoted and stored at -20 °C and diluted to the desired final concentration in DMEM/F12 at the time of use. 3-Methyladenosine (3-MA, Sigma Aldrich, St Louis, MO) was used at a concentration of 50 μmol/L. The final concentration of DMSO in the growth media was less than 0.01%.

Cell viability analysis

MTT assays were performed to assess sensitivity of the cells to the drug. Cells in the log growth phase were seeded in 96-well microplates at a density of 2×10^4 cells in 100 μL media per well. The next day, the cells were treated with various concentrations of NVP-BEZ235 for 24, 48, or 72 h. A control group and a zero adjustment group were also included. Ten microliters of MTT solution (5 mg/mL; Sigma Aldrich, St Louis, MO, USA) was added 4 h before the end of the incubation period, and the reaction was terminated by the addition of 100 μL 10% acidified sodium dodecyl sulfate. The absorbance was measured at 570 nm using an automatic multiwell spectrophotometer (Bio-Tek Instruments, Vermont, USA).

Radiation treatment and clonogenic survival assay

The cells were seeded in six-well plates at a density of 2×10^2 cells per well. After overnight incubation, the cells were pretreated with 50 μmol/L 3-MA and 10 nmol/L NVP-BEZ235 for 12 h and irradiated with 6-MV X-rays from a linear accelerator (PRIMUS, DE, Siemens A&D LD, Nelson Avenue Concord, USA) at a dose rate of 198 cGy/min. Colonies were grown for two weeks until there was visible colony formation. The plates were washed with phosphate-buffered saline (PBS), and the colonies were fixed with methanol for 10 min and stained with 0.5% crystal violet (Sigma Aldrich). The number of colonies with at least 50 cells was counted. The surviving fraction (SF) was calculated as: mean colony count/inoculated cell count×plating efficiency. The sensitization enhancement ratio (SER) was determined by taking the ratio at the mean lethal dose (*ie*, the control radiation dose divided by the NVP-BEZ235-treated radiation dose). SER values greater than 1 indicated an enhancement of radiosensitivity.

Immunofluorescence

The SU-2 cells were plated in six-well plates and treated with 10 nmol/L concentration of NVP-BEZ235 and 8 Gy dose of IR for 24 h. After these treatments, the cells were fixed by incubating in freshly prepared 4% paraformaldehyde solution for 10 min at 4 °C. Following the PBS wash, the cells were blocked in a blocking buffer (1% bovine serum albumin, 0.1% Triton X-100) for 30 min at 37 °C. The cells were then incubated overnight with the rabbit anti–human light chain 3 antibody (LC3) (1:200, Abcam) diluted with the blocking buffer (1:200) in a humidified chamber. After 24 h, the cells were incubated with a secondary antibody (1:200) conjugated to Alexa 488 (Invitrogen) for 1 h at room temperature. Next, the slides were mounted by using a fluorescent mounting medium (Dako) and immediately observed with a confocal microscope to identify the formation of autophagosomes. For the monodansylcadaverine (MDC) staining and LysoTracker Red (LTR) dye

uptake assay, the cells were incubated using the same culture conditions and treated with either 50 μmol/L MDC or LTR for 30 min at 37 °C. After washing with PBS, the cells were fixed with methanol for 10 min. Next, the slides were mounted with the fluorescent mounting medium and observed with a Leica DMIRB inverted fluorescence microscope. For Hoechst 33258 staining, the SU-2 cells were harvested 48 h after IR. The cells were washed and suspended in PBS. The Hoechst 33258 fluorescent dye was added, and the reaction was allowed to proceed in the dark at room temperature for 15 min. Morphological nuclear changes were observed and captured with the Leica DMIRB inverted fluorescence microscope.

Western blot analysis

After treatments as mentioned above, the cells were washed with ice-cold PBS, lysed with a lysis buffer (Beyotime, Haimen, China), and centrifuged at 12000×*g* for 15 min. Supernatants were collected, and the total protein concentration was quantified using the bicinchoninic acid assay kit (Thermo, Rockford, USA). Equal amounts of protein (40 μg) were fractionated by performing 10% sodium dodecyl sulfate-polyacrylamide gel electrophoresis (SDS-PAGE; Bio-Rad) and transferred to 0.45 μm nitrocellulose transfer membranes (Whatman). After blocking with 5% skim milk at room temperature for 1 h, the membranes were incubated with primary antibodies against rabbit anti-LC3 (1:1000; Abcam), mouse anti-Bcl-2 (1:500; Abcam), rabbit anti-BH3 interacting-domain death agonist (BID) (1:1000; Abcam), rabbit anti-Bcl-2-associated X protein (Bax) (1:1000; Cell Signal), rabbit anti-active caspase-3 (1:1000; Abcam), mouse anti-cyclin A (1:750; Abcam), rabbit anti-cyclin B1 (1:5000; Abcam), rabbit anti-cyclin D1 (1:200; Abcam), mouse anti-RAD51 (1:1000; Abcam), and mouse anti-β-actin (1:1000; Cell Signal) at 4 °C for 24 h. The membranes were washed three times with TBST buffer (20 mmol/L Tris-buffered saline and 0.1% Tween 20) for 1 h before incubation with a rabbit or mouse secondary antibody at room temperature. After washing with the TBST buffer, the membranes were scanned with the Odyssey Infrared Imaging System (LI-COR).

Annexin V-fluorescein isothiocyanate/propidium iodide staining

The apoptotic cells were quantified (percentage) using an annexin V-fluorescein isothiocyanate (FITC)/propidium iodide (PI) kit (KeyGEN, Nanjing, China) and detected by flow cytometry. SU-2 cells were harvested 48 h after treatment with IR. Next, the cells were resuspended in the binding buffer (10 mmol/L Hepes, 140 mmol/L NaCl, and 2.5 mmol/L $CaCl_2$; pH 7.4) and incubated with annexin V-FITC/PI in the dark for 15 min. Five thousand cells per sample were analyzed using the FACSCalibur flow cytometer (Epics-XL, Beckman)[9, 10]. Cells in the earlier stages of apoptosis stained positive for annexin V-FITC, whereas those in the later stages of apoptosis stained positive for both annexin V-FITC and PI.

Cell cycle analysis

Cell cycle status was determined by measuring cellular DNA content after staining with PI (KeyGEN, Nanjing, China). The cells were collected after centrifugation for 5 min and fixed in 70% cold ethanol at -20 °C overnight. The next day, the cells were resuspended and treated with RNase A at 37 °C for 30 min and stained with 5 μL PI in the dark at room temperature for 30 min. The samples were subsequently analyzed with the FACSCalibur flow cytometer.

Comet assay

DNA repair in SU-2 cells was assessed using a comet assay. Slides were dipped in 1% normal–melting point agarose/PBS (Sigma Aldrich) and air-dried to thin films. The cells were harvested and resuspended in PBS and quickly mixed with 0.8% low–melting point agarose/PBS (Sigma Aldrich). A coverslip was added on top of each slide, and the slides were placed at 4 °C for 10 min to allow the agarose to solidify. After gel formation, the coverslips were gently removed and the gel was overlaid with an additional 1% normal-melting point agarose/PBS and allowed to solidify. The slides were then submerged in freshly prepared alkaline lysis buffer [4 mol/L NaCl, 500 mmol/L Na_2-ethylenediaminetetraacetic acid (EDTA), 500 mmol/L Tris-HCl, 1% sodium N-lauroyl sarcosinate, 1% Triton X-100, and 10% DMSO, pH 10] at 4 °C for 1 h and kept in the dark. Next, the slides were placed in freshly prepared electrophoresis buffer (1 mmol/L Na_2-EDTA and 300 mmol/L NaOH, pH 13) at 4 °C for 20 min to allow DNA unwinding and the expression of alkali-labile sites. The samples were electrophoresed at 25 V and 300 mA at 4 °C for 30 min. After electrophoresis, the slides were neutralized in 0.4 mol/L Tris, pH 7.5, for 5 min and fixed with methanol for 10 min. Finally, the slides were stained with GelRed and observed with a fluorescence microscope. The entire procedure was conducted in dim light to avoid additional DNA damage. DNA damage for each cell was quantified as follows: the ratio of maximum total length divided by the length of the comet tail (*ie*, maximum total length − head diameter).

Statistical analysis

The mean and standard deviation (mean±SD) were calculated for each parameter. The quantitative data were analyzed at least three times. The critical level for rejection of the null hypothesis was a *P*-value of 5%. All of the analyses were performed with GraphPad Prism 5.0.

Results

NVP-BEZ235 inhibits GSC proliferation and enhances radiosensitivity

The MTT assay showed that NVP-BEZ235 effectively suppressed glioma cell growth when used at nanomolar concentrations (Figure 1A). The radiosensitization of GSCs was determined by performing the clonogenic assay after the treatment of cells with a combination of IR (0 Gy to 8 Gy) and NVP-BEZ235 (10 nmol/L; the concentration that produced an inhibition rate lower than 10% when given alone). The inhibition of the PI3K/mTOR signaling pathway is associated with the induction of autophagy[24–26]. Therefore, we used 3-MA (50 μmol/L), which blocks autophagy at an early stage[27], before

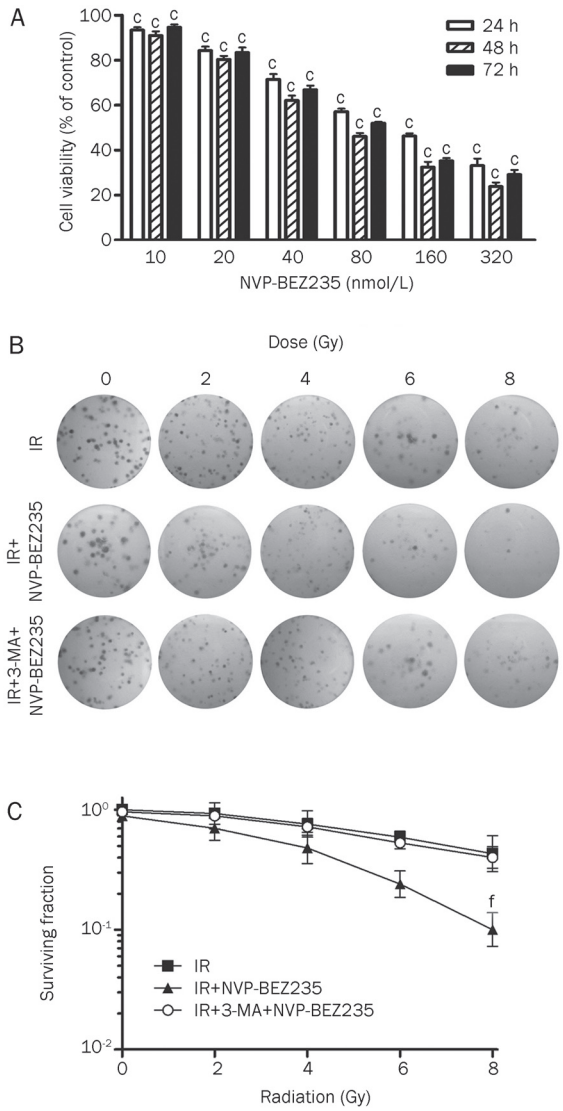

Figure 1. NVP-BEZ235 inhibits GSC proliferation and enhances radiosensitivity. (A) SU-2 cells were treated with increasing concentrations of NVP-BEZ235 for 24, 48, or 72 h and subjected to MTT assay. The plot depicts the percentage growth of the NVP-BEZ235-treated cells compared with that of the untreated control cells (the viability of the untreated control cells was considered as 100%). (B) Clonogenic survival assay in SU-2 cells treated with radiation alone (0 Gy to 8 Gy), radiation plus NVP-BEZ235 (10 nmol/L), or radiation plus 3-MA (50 μmol/L) and NVP-BEZ235 (10 nmol/L). (C) Clonogenic survival curves for (B). Mean±SD. n=3. ^{c}P<0.01 compared with the control group, ^{f}P<0.01 compared with the IR-alone group.

NVP-BEZ235 and IR treatments. As a result, cells treated with IR and NVP-BEZ235 produced a reduced number of colonies compared with the group that was treated with IR-alone, and the combination of 3-MA and NVP-BEZ235 depressed radiosensitivity (Figure 1B). We used Student's *t*-test to analyze the SF values and observed that clonogenicity of SU-2 cells treated with IR and NVP-BEZ235 was significantly reduced in an ionization-dose dependent manner (Figure 1C). Treatment with IR and NVP-BEZ235 resulted in a SER of 1.66 (P<0.01, Student's *t*-test, n=3) compared with IR treatment alone. The SER with the addition of both 3-MA and NVP-BEZ235 to the IR treatment was 0.95 compared with that for IR treatment alone. Therefore, NVP-BEZ235 treatment significantly increased radiation sensitivity in GSCs, and the inhibition of autophagy by 3-MA blocked NVP-BEZ235-mediated radiosensitization.

NVP-BEZ235-mediated radiosensitization increases induction of autophagy

We studied the cleavage of the microtubule-associated protein LC3, a specific molecular marker of autophagosomes, to determine whether NVP-BEZ235-mediated radiosensitization would result from autophagy induction[28]. Importantly, LC3 can be detected as LC3-I (cytosolic) and LC3-II (membrane-bound and enriched in the autophagic vacuole fraction) forms. We examined the localization of LC3 by indirect immunofluorescence microscopy. By performing fluorescence microscopy experiments, a more punctate pattern of LC3 immunoreactivity was observed in SU-2 cells that received NVP-BEZ235 treatment or co-treatment, suggesting an increase in the formation of autophagic vacuoles (Figure 2A, top). In contrast, cells in the control and IR-alone groups showed a diffuse distribution of LC3 immunoreactivity. MDC has been shown to be a useful tracer for autophagic vesicles[29]. We stained SU-2 cells with MDC and LTR, a lysosome indicator, and observed the staining patterns using a fluorescence microscope to monitor the autophagic/lysosomal events. The SU-2 cells that were treated with NVP-BEZ235 alone or with NVP-BUZ235 and IR showed an increased number of MDC-positive vesicles in the cytoplasm, particularly in the perinuclear regions (Figure 2A, middle), which also had more LTR-positive dots (Figure 2A, bottom) This increase suggests that there is formation of autophagic lysosomes and an increase in the induction of autophagy. Changes in the protein levels of LC3-I and LC3-II in GSCs with the same treatments as described above were further confirmed by performing western blot analysis (Figure 2B). The quantification of the percentage of LC3-I and LC3-II expression in each of the treatment groups (Figure 2C) showed an apparent increase in the conversion of LC3-I to LC3-II in SU-2 cells that received the combined treatment. Collectively, these data suggest that the mechanism of NVP-BEZ235-mediated radiosensitization involves autophagy induction.

Induction of GSC apoptosis by co-treatment with IR and NVP-BEZ235

Autophagy and apoptosis together induce cell death[30] and enhance radiosensitivity[31]. Apoptosis can also be induced via enhanced autophagy[32]. Because the co-treatment with IR and NVP-BEZ235 triggered autophagy, we next assessed whether the combination therapy could induce apoptosis in GSCs. The apoptosis level in GSCs was significantly increased by the combined treatment with IR and NVP-BEZ235 as demonstrated by a number of indicators for cellular apoptosis: increased activation of BID, Bax, active caspase-3 and decreased levels of Bcl-2 (Figure 3A and 3B). Annexin V-conjugated FITC and PI staining was performed to measure the percentage of apop-

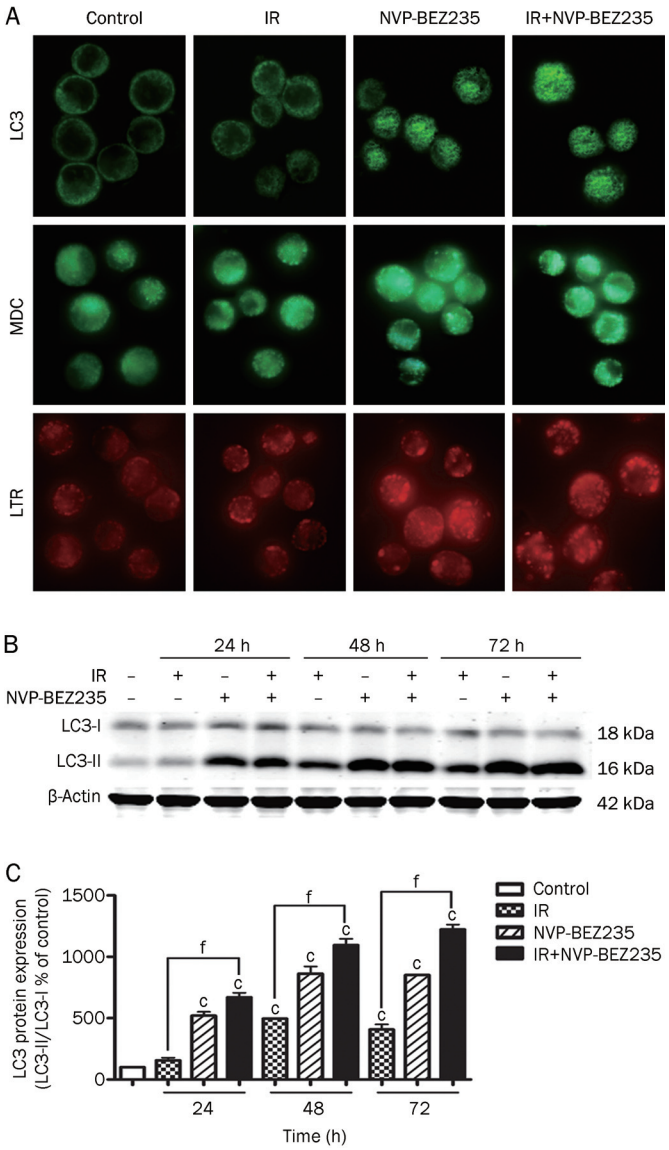

Figure 2. NVP-BEZ235-mediated radiosensitization increases autophagy induction. (A) SU-2 cells were treated with NVP-BEZ235 (10 nmol/L) for 12 h and then harvested 24 h after treatment with IR (8 Gy), and analyzed for LC3 expression (top) or the formation of autophagolysosomes by using MDC (middle) and LTR (bottom) by immunofluorescence analysis (600×magnification). (B) The cells were treated with IR and NVP-BEZ235 and analyzed for LC3 and β-actin expression by Western blot analysis. β-Actin was used as a loading control. (C) Quantification of LC3 protein expression in SU-2 cells treated by indicated treatments after normalization with β-actin levels. Mean±SD. n=3. ^{c}P<0.01 compared with the control group. ^{f}P<0.01 compared with the IR-alone group.

tosis in each treatment group to confirm these observations. The groups that received IR or NVP-BEZ235 treatments alone showed a slight increase in the apoptosis level compared with the control group; however, apoptosis in the co-treated cells was approximately 45-times greater than that noted in the matched untreated cells (Figure 3C and 3D). We stained the nuclei of the treated GSCs with Hoechst 33258 to determine the incidence of apoptosis morphologically. Representative microphotographs showed that morphological characteristics of apoptosis, such as chromatin condensation and nuclear fragmentation, were evident in SU-2 cells treated with both IR (8 Gy) and NVP-BEZ235 (10 nmol/L). All of these data were obtained within 48 h after IR. However, the co-treatment for 24 and 72 h did not show a significant increase in apoptosis compared with the other groups (data not shown). Therefore, NVP-BEZ235-mediated radiosensitization can increase the rate of cellular apoptosis.

G_1 phase block induced by IR and NVP-BEZ235

We next analyzed the effect of NVP-BEZ235 on cell-cycle progression in GSCs. Forty-eight hours after IR, there was a significant increase in the number of cells in the G_1 phase in the co-treated group (71.5%±2.7%) compared with the control group (47.7%±1.2%) (Figure 4A and 4B). This increase suggests that NVP-BEZ235 treatment induced a cell-cycle arrest in the G_1 phase. To determine how NVP-BEZ235 induces G_1 arrest in GSCs, we examined the expression of endogenous cyclins in SU-2 cells after 48 h of treatment with IR (8 Gy) and NVP-BEZ235 (10 nmol/L). Cyclin A is involved in meiotic progression and has markedly lower expression in cells arrested in the G_1 phase[33–35]. Cyclin D1 is a key regulator of the G_1 to S phase progression and is aberrantly expressed in numerous human cancers[36]. The inhibition of cyclin D1 function results in G_1 phase arrest, whereas the regulation of G_2/M phases primarily depends on cyclin B1 function[37]. The results of the Western blot analysis showed that in SU-2 cells treated with NVP-BEZ235, the expression levels of cyclin A and D1 were reduced, but there was only a slight effect on cyclin B1 levels (Figure 4C). The results of the densitometric analysis showed that the levels of cyclin A and D1 were reduced to 64% and 56% of the control, respectively (Figure 4D). Based on these results, we conclude that NVP-BEZ235-mediated downregulation of cyclin A and cyclin D1, which led to G_1 arrest. Therefore, combination therapy in GSCs can induce G_1 arrest by inhibiting the expression of cyclin proteins.

NVP-BEZ235 impairs the repair of radiation-induced DNA damage in GSCs

Because DNA repair is an important mechanism involved in radioresistance, we determined the effects of NVP-BEZ235 on IR-induced cellular DNA damage using the alkaline comet assay[38]. In this study, we measured DNA damage in GSCs at various time points after IR. DNA damage was determined by measuring the tail length of the comet with a microscope. There was no obvious difference in DNA damage between the IR-alone group (8 Gy) and the co-treated group (10 nmol/L NVP-BEZ235 with 8 Gy of IR) immediately after irradiation. However, DNA damage, as reflected by the tail length of the comet, was more severe in the co-treated group than in the IR-alone group at 6 h and 18 h after irradiation (Figure 5A). The data are presented as the mean±SD from at least 50 cells or comets from one single experiment. Each group was analyzed in triplicate (Figure 5B). Thus, NVP-BEZ235-treatment

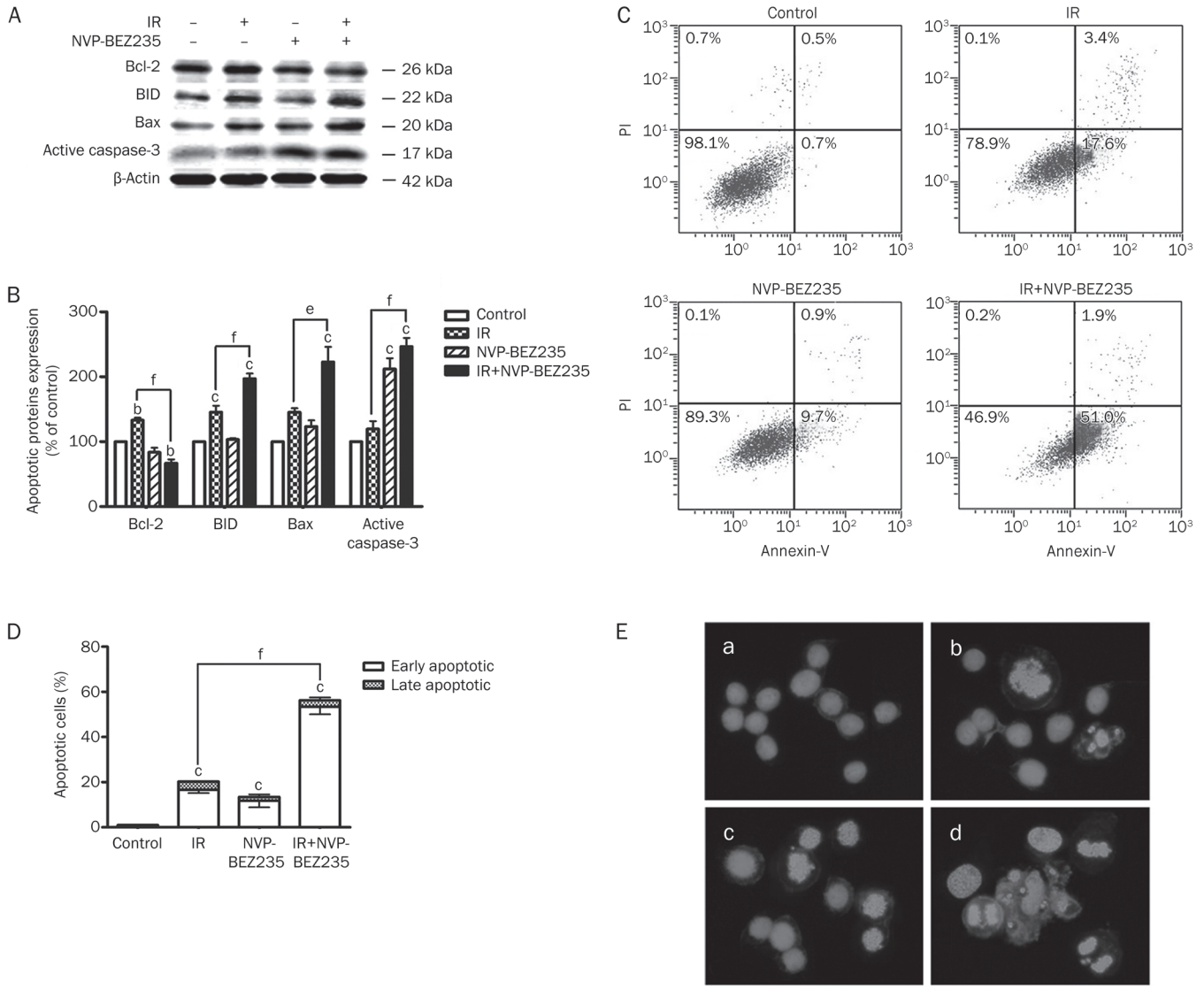

Figure 3. Induction of GSC apoptosis by co-treatment with IR and NVP-BEZ235. (A) SU-2 cells were collected after 48 h of treatment with IR (8 Gy) and NVP-BEZ235 (10 nmol/L), protein lysates were resolved by SDS-PAGE, and immunoblotted with antibodies for Bcl-2, BID, Bax, and active caspase-3. Equal protein loading was confirmed by blotting for β-actin. (B) Quantification of apoptotic proteins expression in SU-2 cells treated by IR and NVP-BEZ235 treatments after normalization with β-actin levels. (C) After treatment with IR and NVP-BEZ235, the cells were stained with annexin V-FITC/PI. The co-treated group demonstrated a dramatic increase in the percentage of apoptotic cells compared with the groups that were untreated (control), treated with IR-alone, or treated with NVP-BEZ235-alone. (D) The quantification of the percentage of apoptotic cells result from (C). (E) The SU-2 cell nuclei were stained with Hoechst 33258 to detect apoptosis morphologically (400×magnification), a) control group; b) IR-alone group; c) NVP-BEZ235-alone group; d) co-treated group. Microphotographs are shown as representative results from three independent experiments. Mean±SD. n=3. $^{b}P<0.05$, $^{c}P<0.01$ compared with the control group. $^{e}P<0.05$, $^{f}P<0.01$ compared with the IR-alone group.

prevented the repair of IR-induced DNA damage. Tumor radiosensitivity was also associated with the expression of genes involved in the cellular response to radiation damage. One such gene, RAD51, is upregulated during the repair of DNA double-strand breaks (DSBs) induced by IR[39]. One of the first cellular responses to DSBs is the phosphorylation of H2AX (γ-H2AX), although γ-H2AX could be eliminated by a PI3K inhibitor. Paull *et al* provided further evidence for the involvement of phosphoinositide 3-kinases in H2AX activation[40]. We studied the DNA damage marker, γ-H2AX, by immunofluorescence to observe the formation of dynamic foci during DNA repair, but the results were not conclusive. Next, we detected RAD51 expression by performing western blot analysis of GSCs after different treatments. IR induced the upregulation of RAD51 expression in GSCs. However, in contrast to the elevation of RAD51 expression in cells treated with IR alone, NVP-BEZ235 pretreatment effectively attenuated the upregulation of RAD51 expression that was induced by IR (Figure 5C and 5D). This attenuation indicates that NVP-BEZ235 treatment overcame the upregulation of RAD51

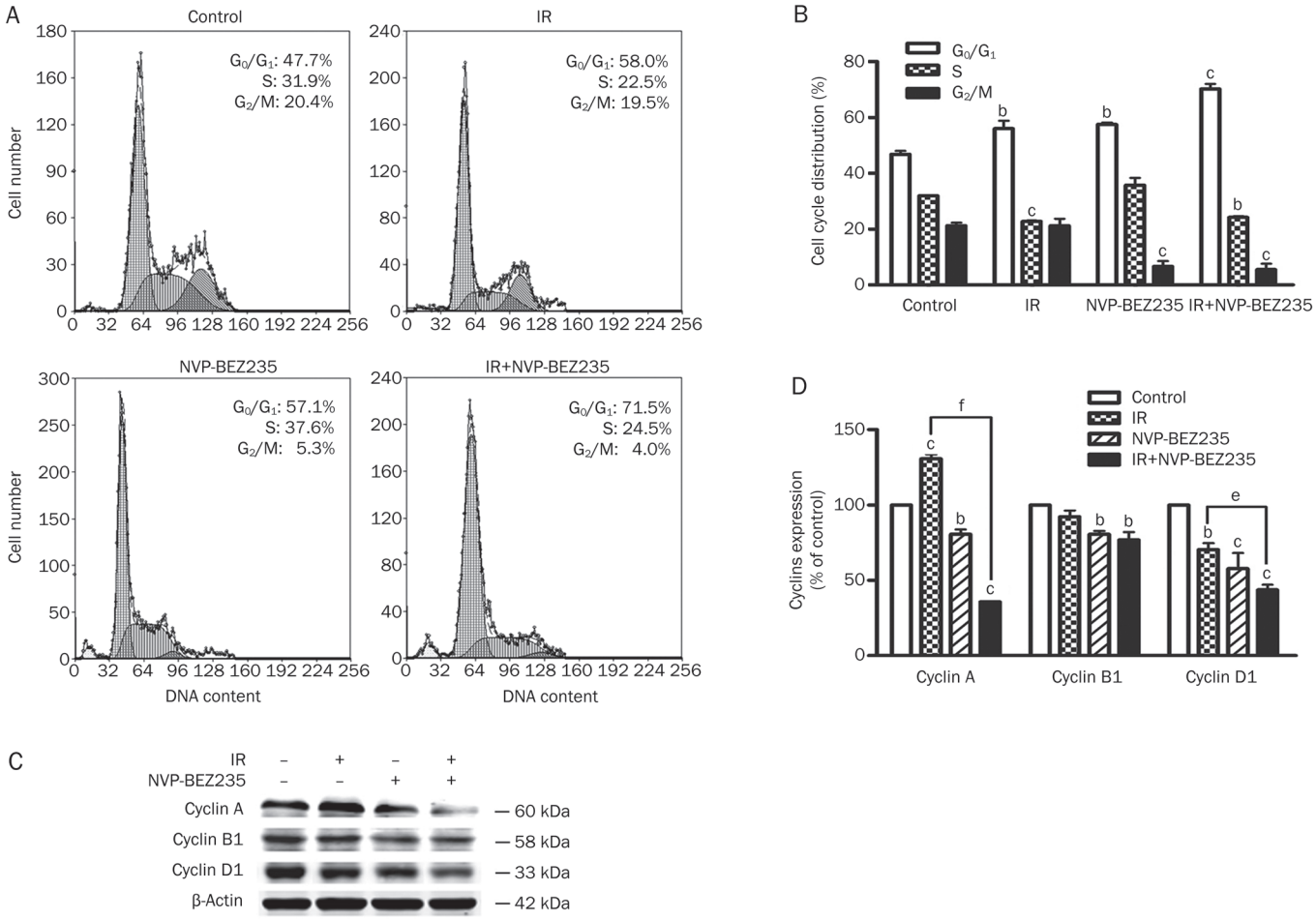

Figure 4. G_1 phase blockade induced by IR and NVP-BEZ235 treatments. (A) SU-2 cells were treated with IR (8 Gy) and NVP-BEZ235 (10 nmol/L) and harvested 48 h after IR. Cellular DNA content was determined by staining with a hypotonic PI solution. (B) Quantification of cell-cycle distribution in SU-2 cells. (C) Western blot analysis of cyclins in GSCs. SU-2 cells were harvested 48 h after IR. (D) The quantitation of protein expression in response to IR and NVP-BEZ235 treatments after normalization with β-actin levels. Mean±SD. n=3. ^bP<0.05, ^cP<0.01 compared with the control group. ^eP<0.05, ^fP<0.01 compared with the IR-alone group.

expression induced by IR. Therefore, NVP-BEZ235 can effectively counteract the repair of radiation-induced DNA damage in GSCs.

Discussion

The overall goals of this study were to investigate the radiosensitizing effect of a novel dual PI3K/mTOR inhibitor in GSCs and to further understand the molecular mechanisms of its action. We demonstrated for the first time that the significant radiosensitization ability of NVP-BEZ235 in GSCs is attributed to its cumulative antitumor effects, including autophagy induction, apoptosis, cell cycle arrest, and prevention of DNA repair.

The PI3K/mTOR pathway is a key regulator of cell growth processes. This signaling pathway is frequently deregulated in various malignancies, including GMB[11, 41]. Thus, targeting the PI3K/mTOR pathway is an attractive strategy for the development of therapeutic agents against GMB. This pathway is a prime target in radiotherapy, and inhibition of this cascade can induce autophagy and enhance the radiosensitivity of tumor cells. In fact, the dual PI3K/mTOR inhibitor NVP-BEZ235 exhibits promising effects against various tumors[42–45]. However, to date, research has not yet focused on the radiosensitization efficacy of NVP-BEZ235 in GSCs, which are a small subpopulation of GBM that exhibit higher radioresistance. In our study, as evidenced by the nanomolar range of half maximal inhibitory concentration values, NVP-BEZ235 can effectively block GSC proliferation. NVP-BEZ235 also had a prodifferentiation effect on A172 cells, which is consistent with previously published research[21]. We adopted a combination strategy and observed that NVP-BEZ235 is also a potent radiosensitizer of GSCs; this is based on the results of two gold standard techniques used to determine cellular radiosensitivity (*ie*, clonogenic and comet assays, for studying the cellular and molecular aspects, respectively). The radiosensitizing activity of NVP-BEZ235 occurred mainly through autophagy induction. Autophagy is a dynamic process of protein degradation and is considered an essential cellular

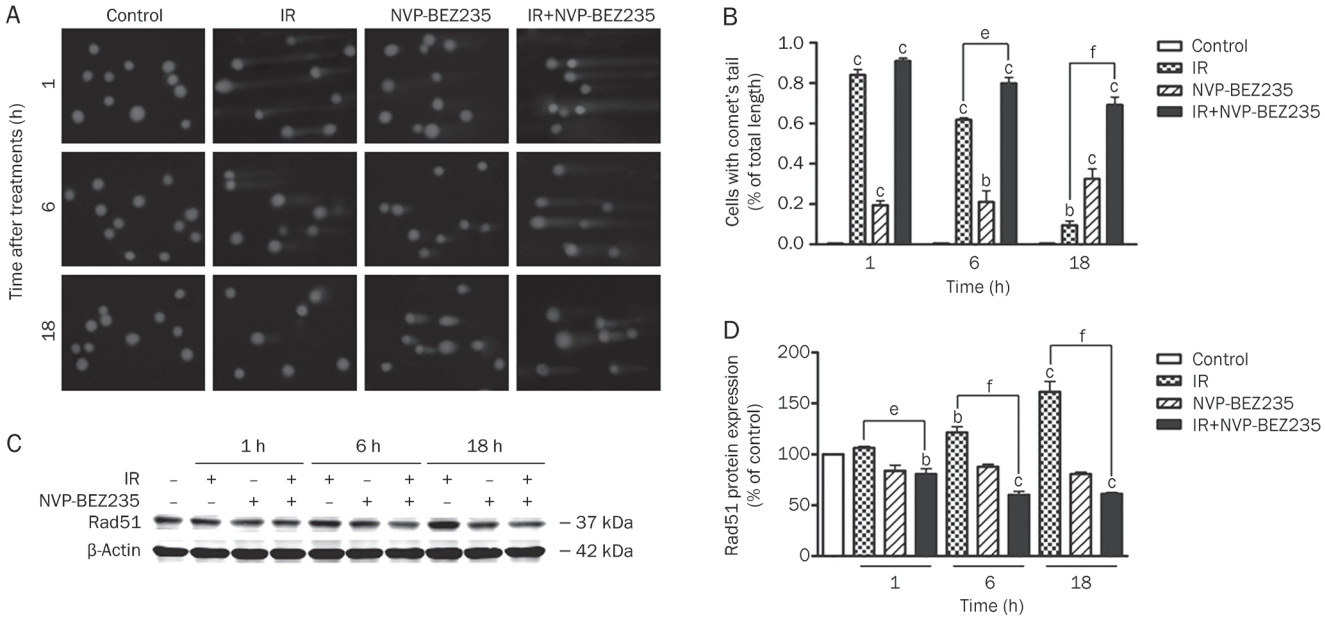

Figure 5. NVP-BEZ235 impairs the repair of radiation-induced DNA damage in GSCs. (A) GSCs were treated with IR (8 Gy) and NVP-BEZ235 (10 nmol/L) and harvested at 1, 6, and 18 h after IR. The alkaline comet assay was performed to determine treatment-induced DNA damage. Representative images of SU-2 cells at indicated time points after various treatments are shown (400×magnification). (B) The quantification of the percentage of cells with comet tails at different time points. (C) Cell lysates were analyzed by Western blot analysis with the indicated antibodies. (D) The relative abundance of each band to β-actin levels was quantified, and the control levels were set at 100%. Mean±SD. n=3. ^{b}P<0.05, ^{c}P<0.01 compared with the control group. ^{e}P<0.05, ^{f}P<0.01 compared with the IR-alone group.

process[46]. Whether autophagy is a survival mechanism or a cause of cell death remains uncertain. Sometimes, autophagy induces the death of damaged cells, and yet at other times, autophagy confers protection[47]. Indeed, autophagy induction functions as a pro-death mechanism (also called type II programmed cell death) in different tumors[48–50]. Treatment with NVP-BEZ235 increased autophagy, as measured by studying LC3-I to LC3-II conversion over an extended period of treatment. The results of the immunofluorescence analysis further confirmed the formation of autolysosomes, although basal autophagic activity in the untreated and IR-treated cells was not detectable[9, 23]. Therefore, autophagy induction could be a direct response of GSCs to the blockade of signals necessary for triggering radioresistance. The radiosensitization efficiency of NVP-BEZ235 was further substantiated by performing cellular apoptosis assays. As shown by both annexin V-FITC/PI and Hoechst 33258 staining, apoptosis in co-treated cells was more frequent than that in the other groups at 48 h after IR. However, co-treatment for 24 h and 72 h resulted in no significant difference in apoptosis compared to that observed with IR-alone treatment. Among the different indicators of cellular apoptosis, the Bcl-2 family of proteins can tightly control both apoptosis and autophagy; they inhibit apoptosis by binding with Bax/Bcl-2 homologous antagonist/killer and apoptotic protease activating factor and suppress autophagy by binding with Beclin-1, a protein involved in the initial stages of autophagy[51]. Indeed, the level of Bcl-2 proteins in the IR-alone group was significantly higher than that in the co-treatment group (P<0.001). Furthermore, results from the flow cytometric analysis demonstrated that the combination strategy induced a G_1 phase block. This cell-cycle arrest in the G_1 phase may be related to the downregulation of endogenous cyclin A and D1.

In summary, inhibition of the PI3K/mTOR signaling pathway in combination with IR is a potential therapeutic strategy for treating GBM. The radiosensitization efficiency of NVP-BEZ235 is achieved by impairing the capacity for DNA repair in the early stage and inducing massive autophagic and apoptotic responses in addition to cell-cycle arrest. Based on these observations, further experimentation with animal models and clinical trials should be explored.

Acknowledgements

This work was supported by grants from the National Natural Science Foundation of China (Grant Nos 30873052, 81072656, 81102466), Jiangsu Province's outstanding Medical Academic Leader program (No LJ201139) and Priority Academic Program Development of Jiangsu Higher Education Institutions, PAPD, Jiangsu Province's Key Medical Department in 2011.

Author contribution

Zhong-qin LIANG designed research; Wen-juan WANG, Lin-mei LONG, Neng YANG, Qing-qing ZHANG, Wen-jun JI, Jiang-hu ZHAO, Zhong WANG, and Gang CHEN performed research; Wen-juan WANG analyzed data; Wen-juan WANG and Zheng-hong QIN wrote the paper.

References

1 Tunici P, Irvin D, Liu G, Yuan X, Zhaohui Z, Ng H, *et al*. Brain tumor stem cells: new targets for clinical treatments? Neurosurg Focus 2006; 20: E27.
2 Gupta T, Nair V, Paul SN, Kannan S, Moiyadi A, Epari S, *et al*. Can irradiation of potential cancer stem-cell niche in the subventricular zone influence survival in patients with newly diagnosed glioblastoma? J Neurooncol 2012; 109: 195–203.
3 Singh SK, Hawkins C, Clarke ID, Squire JA, Bayani J, Hide T, *et al*. Identification of human brain tumour initiating cells. Nature 2004; 432: 396–401.
4 Qiu B, Zhang D, Tao J, Wu A, Wang Y. A simplified and modified procedure to culture brain glioma stem cells from clinical specimens. Oncol Lett 2012; 3: 50–4.
5 Jamal M, Rath BH, Tsang PS, Camphausen K, Tofilon PJ. The brain microenvironment preferentially enhances the radioresistance of CD133 (+) glioblastoma stem-like cells. Neoplasia 2012; 14: 150–8.
6 Bao S, Wu Q, McLendon RE, Hao Y, Shi Q, Hjelmeland AB, *et al*. Glioma stem cells promote radioresistance by preferential activation of the DNA damage response. Nature 2006; 444: 756–60.
7 Lima FR, Kahn SA, Soletti RC, Biasoli D, Alves T, da Fonseca AC, *et al*. Glioblastoma: therapeutic challenges, what lies ahead. Biochin Biophys Acta 2012; 1826: 338–49.
8 Wu J, Lai G, Wan F, Xiao Z, Zeng L, Wang X, *et al*. Knockdown of checkpoint kinase 1 is associated with the increased radiosensitivity of glioblastoma stem-like cells. Tohoku J Exp Med 2012; 226: 267–74.
9 Zhuang W, Li B, Long L, Chen L, Huang Q, Liang Z. Induction of autophagy promotes differentiation of glioma-initiating cells and their radiosensitivity. Int J Cancer 2011; 129: 2720–31.
10 Zhuang W, Li B, Long L, Chen L, Huang Q, Liang ZQ. Knockdown of the DNA-dependent protein kinase catalytic subunit radiosensitizes glioma-initiating cells by inducing autophagy. Brain Res 2011; 1371: 7–15.
11 Serra V, Markman B, Scaltriti M, Eichhorn PJ, Valero V, Guzman M, *et al*. NVP-BEZ235, a dual PI3K/mTOR inhibitor, prevents PI3K signaling and inhibits the growth of cancer cells with activating PI3K mutations. Cancer Res 2008; 68: 8022–30.
12 Prevo R, Deutsch E, Sampson O, Diplexcito J, Cengel K, Harper J, *et al*. Class I PI3 kinase inhibition by the pyridinylfuranopyrimidine inhibitor PI-103 enhances tumor radiosensitivity. Cancer Res 2008; 68: 5915–23.
13 Gallia GL, Rand V, Siu IM, Eberhart CG, James CD, Marie SK, *et al*. PIK3CA gene mutations in pediatric and adult glioblastoma multiforme. Mol Cancer Res 2006; 4: 709–14.
14 Gomez-Pinillos A, Ferrari AC. mTOR signaling pathway and mTOR inhibitors in cancer therapy. Hematol Oncol Clin North Am 2012; 26: 483–505.
15 Wallin JJ, Edgar KA, Guan J, Berry M, Prior WW, Lee L, *et al*. GDC-0980 is a novel class I PI3K/mTOR kinase inhibitor with robust activity in cancer models driven by the PI3K pathway. Mol Cancer Ther 2011; 10: 2426–36.
16 Fokas E, Im JH, Hill S, Yameen S, Stratford M, Beech J, *et al*. Dual inhibition of the PI3K/mTOR pathway increases tumor radiosensitivity by normalizing tumor vasculature. Cancer Res 2012; 72: 239–48.
17 Liu TJ, Koul D, LaFortune T, Tiao N, Shen RJ, Maira SM, *et al*. NVP-BEZ235, a novel dual phosphatidylinositol 3-kinase/mammalian target of rapamycin inhibitor, elicits multifaceted antitumor activities in human gliomas. Mol Cancer Ther 2009; 8: 2204–10.
18 Mukherjee B, Tomimatsu N, Amancherla K, Camacho CV, Pichamoorthy N, Burma S. The dual PI3K/mTOR inhibitor NVP-BEZ235 is a potent inhibitor of ATM- and DNA-PKCs-mediated DNA damage responses. Neoplasia 2012; 14: 34–43.
19 Fokas E, Yoshimura M, Prevo R, Higgins G, Hackl W, Maira SM, *et al*. NVP-BEZ235 and NVP-BGT226, dual phosphatidylinositol 3-kinase/mammalian target of rapamycin inhibitors, enhance tumor and endothelial cell radiosensitivity. Radiat Oncol 2012; 7: 48.
20 Konstantinidou G, Bey EA, Rabellino A, Schuster K, Maira MS, Gazdar AF, *et al*. Dual phosphoinositide 3-kinase/mammalian target of rapamycin blockade is an effective radiosensitizing strategy for the treatment of non-small cell lung cancer harboring K-RAS mutations. Cancer Res 2009; 69: 7644–52.
21 Sunayama J, Sato A, Matsuda K, Tachibana K, Suzuki K, Narita Y, *et al*. Dual blocking of mTor and PI3K elicits a prodifferentiation effect on glioblastoma stem-like cells. Neuro Oncol 2010; 12: 1205–19.
22 Sunayama J, Matsuda K, Sato A, Tachibana K, Suzuki K, Narita Y, *et al*. Crosstalk between the PI3K/mTOR and MEK/ERK pathways involved in the maintenance of self-renewal and tumorigenicity of glioblastoma stem-like cells. Stem Cells 2010; 28: 1930–9.
23 Huang Q, Zhang QB, Dong J, Wu YY, Shen YT, Zhao YD, *et al*. Glioma stem cells are more aggressive in recurrent tumors with malignant progression than in the primary tumor, and both can be maintained long-term *in vitro*. BMC Cancer 2008; 8: 304.
24 Chiarini F, Grimaldi C, Ricci F, Tazzari PL, Evangelisti C, Ognibene A, *et al*. Activity of the novel dual phosphatidylinositol 3-kinase/mammalian target of rapamycin inhibitor NVP-BEZ235 against T-cell acute lymphoblastic leukemia. Cancer Res 2010; 70: 8097–107.
25 Yang S, Xiao X, Meng X, Leslie KK. A mechanism for synergy with combined mTOR and PI3 kinase inhibitors. PLoS One 2011; 6: e26343.
26 Jaber N, Dou Z, Chen JS, Catanzaro J, Jiang YP, Ballou LM, *et al*. Class III PI3K Vps34 plays an essential role in autophagy and in heart and liver function. Proc Natl Acad Sci U S A 2012; 109: 2003–8.
27 Cerniglia GJ, Karar J, Tyagi S, Christofidou-Solomidou M, Rengan R, Koumenis C, *et al*. Inhibition of autophagy as a strategy to augment radiosensitization by the dual phosphatidylinositol 3-kinase/mammalian target of rapamycin inhibitor NVP-BEZ235. Mol Pharmacol 2012; 82: 1230–40.
28 Kuma A, Matsui M, Mizushima N. LC3, an autophagosome marker, can be incorporated into protein aggregates independent of autophagy: caution in the interpretation of LC3 localization. Autophagy 2007; 3: 323–8.
29 Griffin C, McNulty J, Pandey S. Pancratistatin induces apoptosis and autophagy in metastatic prostate cancer cells. Int Oncol 2011; 38: 1549–56.
30 Zhang M, Jiang M, Bi Y, Zhu H, Zhou Z, Sha J. Autophagy and apoptosis act as partners to induce germ cell death after heat stress in mice. PLoS One 2012; 7: e41412.
31 Kim KW, Moretti L, Mitchell LR, Jung DK, Lu B. Combined Bcl-2/mammalian target of rapamycin inhibition leads to enhanced radiosensitization via induction of apoptosis and autophagy in non-small cell lung tumor xenograft model. Clin Cancer Res 2009; 15: 6096–105.
32 Tai S, Sun Y, Liu N, Ding B, Hsia E, Bhuta S, *et al*. Combination of Rad001 (everolimus) and propachlor synergistically induces apoptosis through enhanced autophagy in prostate cancer cells. Mol Cancer Ther 2012; 11: 1320–31.
33 Frum R, Ramamoorthy M, Mohanraj L, Deb S, Deb SP. MDM2 controls the timely expression of cyclin A to regulate the cell cycle. Mol Cancer Res 2009; 7: 1253–67.
34 Fung TK, Ma HT, Poon RY. Specialized roles of the two mitotic cyclins in somatic cells: cyclin A as an activator of M phase-promoting factor.

Mol Biol Cell 2007; 18: 1861–73.
35 Mori T, Ikeda DD, Fukushima T, Takenoshita S, Kochi H. NIRF constitutes a nodal point in the cell cycle network and is a candidate tumor suppressor. Cell Cycle 2011; 10: 3284–99.
36 Saha A, Halder S, Upadhyay SK, Lu J, Kumar P, Murakami M, *et al*. Epstein-Barr virus nuclear antigen 3C facilitates G_1-S transition by stabilizing and enhancing the function of cyclin D1. PLoS Pathog 2011; 7: e1001275.
37 Mollah ML, Park DK, Park HJ. Cordyceps militaris grown on germinated soybean induces G_2/M cell cycle arrest through down-regulation of cyclin B1 and Cdc25c in human colon cancer HT-29 cells. Evid Based Complement Alternat Med 2012; 2012: 249217.
38 Jayakumar S, Bhilwade HN, Pandey BN, Sandur SK, Chaubey RC. The potential value of the neutral comet assay and the expression of genes associated with DNA damage in assessing the radiosensitivity of tumor cells. Mutat Res 2012; 748: 52–9.
39 Liu Q, Jiang H, Liu Z, Wang Y, Zhao M, Hao C, *et al*. Berberine radiosensitizes human esophageal cancer cells by downregulating homologous recombination repair protein RAD51. PLoS One 2011; 6: e23427.
40 Paull TT, Rogakou EP, Yamazaki V, Kirchgessner CU, Gellert M, Bonner WM. A critical role for histone H2AX in recruitment of repair factors to nuclear foci after DNA damage. Curr Biol 2000; 10: 886–95.
41 Ekman S, Wynes MW, Hirsch FR. The mTOR pathway in lung cancer and implications for therapy and biomarker analysis. J Thorac Oncol 2012; 7: 947–53.
42 Chapuis N, Tamburini J, Green AS, Vignon C, Bardet V, Neyret A, *et al*. Dual inhibition of PI3K and mTORC1/2 signaling by NVP-BEZ235 as a new therapeutic strategy for acute myeloid leukemia. Clin Cancer Res 2010; 16: 5424–35.
43 Roper J, Richardson MP, Wang WV, Richard LG, Chen W, Coffee EM, *et al*. The dual PI3K/mTOR inhibitor NVP-BEZ235 induces tumor regression in a genetically engineered mouse model of PIK3CA wild-type colorectal cancer. PoLS One 2011; 6: e25132.
44 Elfiky AA, Aziz SA, Conrad PJ, Siddiqui S, Hackl W, Maira M, *et al*. Characterization and targeting of phosphatidylinositol-3 kinase (PI3K) and mammalian target of rapamycin (mTOR) in renal cell cancer. J Transl Med 2011; 9: 133.
45 Civallero M, Cosenza M, Marcheselli L, Pozzi S, Sacchi S. NVP-BEZ235 alone and in combination in mantle cell lymphoma: an effective therapeutic strategy. Expert Opin Investig Drugs 2012; 21: 1597-606.
46 Hippert MM, O'Toole PS, Thorburn A. Autophagy in cancer: good, bad, or both? Cancer Res 2006; 66: 9349–51.
47 Zhuang W, Qin Z, Liang Z. The role of autophagy in sensitizing malignant glioma cells to radiation therapy. Acta Biochim Biophys Sin (Shanghai) 2009; 41: 341–51.
48 Mosieniak G, Adamowicz M, Alster O, Jaskowiak H, Szczepankiewicz AA, Wilczynski GM, *et al*. Curcumin induces permanent growth arrest of human colon cancer cells: link between senescence and autophagy. Mech Ageing Dev 2012; 133: 444–55.
49 Natsumeda M, Aoki H, Miyahara H, Yajima N, Uzuka T, Toyoshima Y, *et al*. Induction of autophagy in temozolomide treated malignant gliomas. Neuropathology 2011; 31: 486–93.
50 Altmeyer A, Josset E, Denis JM, Gueulette J, Slabbert J, Mutter D, *et al*. The mTOR inhibitor RAD001 augments radiation-induced growth inhibition in a hepatocellular carcinoma cell line by increasing autophagy. Int J Oncol 2012. doi: 10.3892/ijo.2012.1583.51
Zhou S, Zhao L, Kuang M, Zhang B, Liang Z, Yi T, *et al*. Autophagy in tumorigenesis and cancer therapy: Dr Jekyll or Mr Hyde? Cancer Lett 2012; 323: 115–27.